Novel Single-Source Precursors Approach to Prepare Highly Uniform Bi_2S_3 and Sb_2S_3 Nanorods via a Solvothermal Treatment

Wenjing Lou,[†,‡] Miao Chen,*[,†] Xiaobo Wang,[†] and Weimin Liu[†]

State Key Laboratory of Solid Lubrication, Lanzhou Institute of Chemical Physics, Chinese Academy of Sciences, Lanzhou 730000, P. R. China, and Graduate School of Chinese Academy of Sciences, Beijing 100039, P. R. China

Received October 25, 2006. Revised Manuscript Received December 11, 2006

High-quality Bi_2S_3 and Sb_2S_3 nanorods on a large scale were successfully synthesized by the solvothermal treatment of a novel kind of single-source precursors (SSPs), metal di-*n*-octyl-dithiophosphates ($M[S_2P(OC_8H_{17})_2]_3$, M = Bi, Sb). The X-ray powder diffraction (XRD) patterns show that both of these products belong to the orthorhombic M_2S_3 phase. The experimental results show that the Bi_2S_3 nanorods can be easily prepared in air at ≥140 °C for 5 h in the presence of oleylamine. Transmission electron microscopy (TEM) images show the rodlike appearance of Bi_2S_3 with a diameter of 7−21 nm and length of several hundred nanometers under the various reaction conditions. The effects of reaction parameters, such as reaction time, temperature, and concentration of the precursor, on the growth of nanorods were discussed in detail. The mechanism of the formation process of the nanorods was proposed. We also demonstrate that this method can be extended to the synthesis of Sb_2S_3 nanorods, which have an average diameter in the range of 45 nm and a length in the range of 1 μm. The optical absorption experiment shows that these nanorods are semiconductor with bandwidth $E_g = 1.67$ eV for Bi_2S_3 and 1.76 eV for Sb_2S_3, both near to the optimum for photovoltaic conversion, suggesting these nanorods could be used in solar energy and photoelectronic applications.

1. Introduction

The V−VI class of materials is of special importance because of their thermoelectric properties.[1] As representatives of V−VI semiconductors, M_2S_3 (M = Bi, Sb) compounds have recently drawn significant interest.[2] Bismuth sulfides (Bi_2S_3) and antimony sulfides (Sb_2S_3) are a kind of layer-structured direct band gap semiconductor that crystallizes in the orthorhombic system (*pbnm* space group).[3] Bi_2S_3 is useful for photodiode arrays or photovoltaics and belongs to the family of solid-state materials with applications in cooling technologies based on the Peltier effect.[4,5] Sb_2S_3 is regarded as a prospective material for solar energy because of its good photoconductivity[6] and has also been used in thermoelectric cooling technologies and optoelectronics in the IR region.[7] A great deal of effort has been devoted to the preparation of Bi_2S_3 and Sb_2S_3 particles and their films.[8]

One-dimensional (1D) semiconductor nanomaterials have attracted considerable interest for scientific research in recent years because of their remarkable electronic, magnetic, optical, catalytic, and mechanical properties and their potential applications in nanodevices.[9] Many methods have been developed to synthesize 1D M_2S_3 nanomaterials, including nanorods, nanoribbons, and nanotubes.[3,4,10] More recently, the single-source precursor (SSP) approach has attracted much more attention because it is possible to tune the size and size distribution of the products by controlling the reaction conditions. In this aspect, several groups have developed some meaningful methods on the preparations of II−VI, IV−VI, and V−VI semiconductor nanocrystals by using metal dialkyldithiocarbamato complexes as precursors.[11] However, these preparation processes often need a relative high temperature, inert ambience, and sealed containers, etc., and the sizes of the resulting nanorods are always in the range of hundreds nanometers even to several micrometerss, which cannot exhibit their special quantum

* Corresponding author. Tel: 86 9314368189. Fax: 86 9318277088. E-mail: miaochen@lzb.ac.cn.
† Lanzhou Institute of Chemical Physics, Chinese Academy of Sciences.
‡ Graduate School of the Chinese Academy of Sciences.

(1) (a) Wang, W.; Poudel, B.; Yang, J.; Wang, D. Z.; Ren, J. F. *J. Am. Chem. Soc.* **2005**, *127*, 13792.(b) Garje, S. S.; Eisler, D. J.; Ritch, J. S.; Afzaal, M.; O'Brien, P.; Chivers, T. *J. Am. Chem. Soc.* **2006**, *128*, 3120.
(2) Wang, J. W.; Li, Y. D. *Mater. Chem. Phys.* **2004**, *87*, 420.
(3) (a) Yu, Y.; Jin, C. H.; Wang, R. H.; Chen, Q.; Peng, L. M. *J. Phys. Chem. B* **2005**, *109*, 18772. (b) Yu, Y.; Wang, R. H.; Chen, Q.; Peng, L. M. *J. Phys. Chem. B* **2005**, *109*, 23312. (c) Yu, Y.; Wang, R. H.; Chen, Q.; Peng, L. M. *J. Phys. Chem. B* **2006**, *110*, 13415.
(4) Ye, C. H.; Meng, G. W.; Jiang, Z.; Wang, Y. H.; Wang, G. Z.; Zhang, L. D. *J. Am. Chem. Soc.* **2002**, *124*, 15180.
(5) Monteiro, O. C.; Trindade, T. J. *J. Mater. Sci. Lett.* **2000**, *19*, 859.
(6) (a) Roy, B.; Chakraborty, B. R.; Bhattacharya, R.; Dutta, A. K. *Solid State Commun.* **1978**, *25*, 973. (b) Savadogo, O.; Mandal, K. C. *Sol. Energy Mater. Sol. Cells* **1992**, *26*, 117.
(7) Hu, H. M.; Mo, M. S.; Yang, B. J.; Zhang, X. J.; Li, Q. W.; Yu, W. C.; Qian, Y. T. *J. Cryst. Growth* **2003**, *258*, 106.
(8) (a) Suarez, R.; Nair, P. K.; Kamat, P. V. *Langmuir* **1998**, *14*, 3236. (b) Mane, R. S.; Sankapal, B. R.; Lokhande, C. D. *Thin Solid Films* **2000**, *359*, 136.
(9) (a) Huang, Y.; Duan, X. F.; Cui, Y.; Lauhon, L. J.; Kim, K. H.; Lieber, C. M. *Science* **2001**, *294*, 1313. (b) Bachtold, A.; Hadley, P.; Nakanishi, T.; Dekker, C. *Science* **2001**, *294*, 1317.
(10) Monteiro, O. C.; Trindade, T.; Park, J. H.; O'Brien, P. *Chem. Vap. Deposition* **2000**, *6*, 230.
(11) (a) Pradhan, N.; Katz, B.; Efrima, S. *J. Phys. Chem. B* **2003**, *107*, 13843. (b) Xie, G.; Qiao, Z. P.; Zeng, M. H.; Chen, X. M.; Gao, S. L. *Cryst. Growth Des.* **2004**, *4*, 513. (c) Mirkovic, T.; Hines, M. A.; Nair, P. S.; Scholes, G. D. *Chem. Mater.* **2005**, *17*, 3451.

10.1021/cm062549o CCC: $37.00
Published on Web 01/23/2007

confinement effects. So it is therefore highly desirable to develop simple and mild methods for large-scale synthesis of single-crystalline M_2S_3 rods with nanoscale sizes.

In this paper, we report a one-step method for synthesizing high-quality single-crystal Bi_2S_3 nanorods by thermal decomposition of $Bi[S_2P(OC_8H_{17})_2]_3$ in the presence of oleylamine at 140−180 °C. Although $Bi[S_2P(OR)_2]_3$ and its analogues have been synthesized and characterized,[12] it is the first time it has been used as a precursor to synthesize Bi_2S_3 nanomaterials. Furthermore, we find that in this process, the preparation parameters, such as reaction time, temperature, and concentration of the precursor, have a great effect on the size and aspect ratio of the products, which can be utilized to tailor the morphology of the products. We have also proved that this method can be easily extended to the synthesis of other V−VI semiconductor nanomaterials; uniform single-crystal Sb_2S_3 nanorods were prepared as an example.

2. Experimental Section

2.1. Materials and Instruments. All chemical reagents used in this experiment were of analytical grade. Bismuth nitrate ($Bi(NO_3)_3 \cdot 5H_2O$), antimony trichloride ($SbCl_3$), ammonium *O*,*O*′-di-*n*-octyl-dithiophosphate, and oleylamine were procured commercially and were used without further purification. The powder X-ray diffraction (XRD) experiments were measured on a RigaKu D/max-RB diffractometer with Ni-filtered graphite-monochromatized Cu Kα radiation ($\lambda = 1.54056$ Å) under 40 kV and 30 mA and scanning between 10 and 90° (2θ). Transmission electron microscopy (TEM) photographs and selected area electron diffraction (SAED) patterns were taken with a JEOL JEM 1200 transmission electron microscope with an accelerating voltage of 100 kV, and high-resolution transmission electron microscopy (HRTEM) studies were carried out on a JEOL JEM 2010 transmission electron microscope with an accelerating voltage of 200 kV. Samples were prepared by first dispersing the products in *n*-hexane by ultrasonication, placing a drop of the suspension on a copper grid, and drying the samples in air for observation. Optical absorption measurements were carried out using an Analytic Jena AG Spectra 50 UV−visible spectrometer at room temperature. Samples for optical measurement were dispersed in *n*-hexane, which was also used as reference. X-ray photoelectron spectra (XPS) were recorded on a PHI-5702 X-ray photoelectron spectrometer with Al Kα X-ray as the excitation source. The results obtained in the XPS analysis were corrected by referencing the C_{1s} line to 284.6 eV.

2.2. Synthesis of Single-Source Precursors. The metal complexes $Bi[S_2P(OC_8H_{17})_2]_3$ and $Sb[S_2P(OC_8H_{17})_2]_3$ were prepared according to the following equation[12] by the reaction of bismuth-(III) nitrate and antimony(III) trichloride with ammonium *O*,*O*′-di-*n*-octyl-dithiophosphate in a mixture solution of water and ethanol in air at room temperature. Apple green liquid of bismuth complexes and buff liquid of antimony complexes could be obtained, which cannot be dissolved in ethanol.

$$M^{3+} + 3NH_4S_2P(OC_8H_{17})_2 \rightarrow M[S_2P(OC_8H_{17})_2]_3 + 3NH_4^+, (M = Bi, Sb)$$

2.3. Typical Synthetic Process of M_2S_3 Nanorods. $Bi[S_2P(OC_8H_{17})_2]_3$ (0.26 g, 0.2 mmol) and oleylamine (5 g) were added to a glass flask with a capacity of 6 mL. After being shaken, a light green transparent solution can be achieved. The reaction solution was then rapidly heated to 160 °C by immersing the glass flask into a hot oil bath. At this temperature, the color of the solution turned to bright yellow-green quickly, and then turned into dark gray in a few seconds, indicating the formation of Bi_2S_3. The reaction mixture was kept at this temperature for 1.5 h, then prolonged heating at 140 °C for 3.5 h to ensure the completeness of the reaction. After the reaction finished, the resulting solution was cooled to room-temperature naturally, and mixed with an excess amount of acetone, which was used to precipitate the formed Bi_2S_3 nanomaterials from the resulting solution. The precipitated dark-gray flocculant was collected by centrifugation and thoroughly washed with absolute ethanol. The achieved black solid was the product. All manipulations in this preparation process were performed in air. A similar process was used to synthesize Sb_2S_3 nanorods. $Sb[S_2P(OC_8H_{17})_2]_3$ (0.2 mmol) was dissolved in 5 g of oleylamine to form a light-yellow solution. The solution was heated to 160 °C, kept there for 1.5 h, and then fixed at 140 °C for 3.5 h. The color of the reaction solution also turned dark gray after several minutes of heating, indicating the formation of Sb_2S_3. The Sb_2S_3 nanorods product was collected in the same manner.

2.4. Synthesis of Bi_2S_3 Nanorods under Various Reaction Conditions. A series of samples prepared at various reaction times were achieved by heating a solution of 0.39 g (0.3 mmol) of $Bi[S_2P(OC_8H_{17})_2]_3$ and 5 g of oleylamine to 160 °C and keeping it at this temperature for 1, 3, 10, 60, 100, and 300 min, respectively. Samples prepared at various reaction temperatures were achieved by heating s solution of 0.3 mmol of $Bi[S_2P(OC_8H_{17})_2]_3$ and 5 g of oleylamine for 5 h at 120, 140, 160, and 180 °C, respectively. Samples prepared at different precursor concentrations were achieved by dissolving 0.1, 0.2, and 0.3 mmol of $Bi[S_2P(OC_8H_{17})_2]_3$ in 5 g of oleylamine, and then heating them to 160 °C and keeping them at this temperature for 5 h. When the heating finished, these resulting solutions were cooled to room temperature naturally and mixed with an excess amount of acetone. The desired products were achieved by centrifugation of the precipitated flocculants and washed with absolute ethanol.

3. Results and Discussion

The TEM image in Figure 1a shows the good quality of the as-prepared Bi_2S_3 nanorods with a length of several hundred nanometers and diameter of 7−12 nm. It is also clearly seen that these size- and shape-monodisperse nanorods arrange into the thermodynamically most favorable structure on the time scale allowed by the evaporating solvent. It is worth noting that these nanorods organize into relatively thick bundle structures as compared to CdS or Ag_2S nanocrystals that tend to spread onto the substrate surface as opposed to crystallizing into three-dimensional superlattices when drop-cast from a suitable solvent;[13] this is due to these nanorods being nanoscale and their sizes being uniform. The XRD pattern of the product (Figure 1b) shows a series of broadening peaks that are typical for materials in the nanoscale. The diffraction peaks can be completely indexed to the orthorhombic phase of Bi_2S_3 (cell constants $a = 11.15$ Å, $b = 11.30$ Å, $c = 3.981$ Å; JCPDS card file 17-320), and no peak attributable to crystalline Bi, S, or oxides of these elements is observed. The XPS analysis (Figure 1c) reveals that the value of the Bi $4f_{7/2}$ and $4f_{5/2}$ peaks are 158.0 and

(12) (a) Lawton, S. L.; Fuhrmeister, C. J.; Haas, R. G.; Jarman, C. S.; Lohmeyer, F. G. *Inorg. Chem.* **1974**, *13*, 135.(b) Ionel, H.; Anamaria, B. R.; Marius, S. *Inorg. Chim. Acta* **1983**, *68*, 87.

(13) Korgel, B. A.; Fitzmaurice, D. *Phys. Rev. Lett.* **1998**, *80*, 3531.

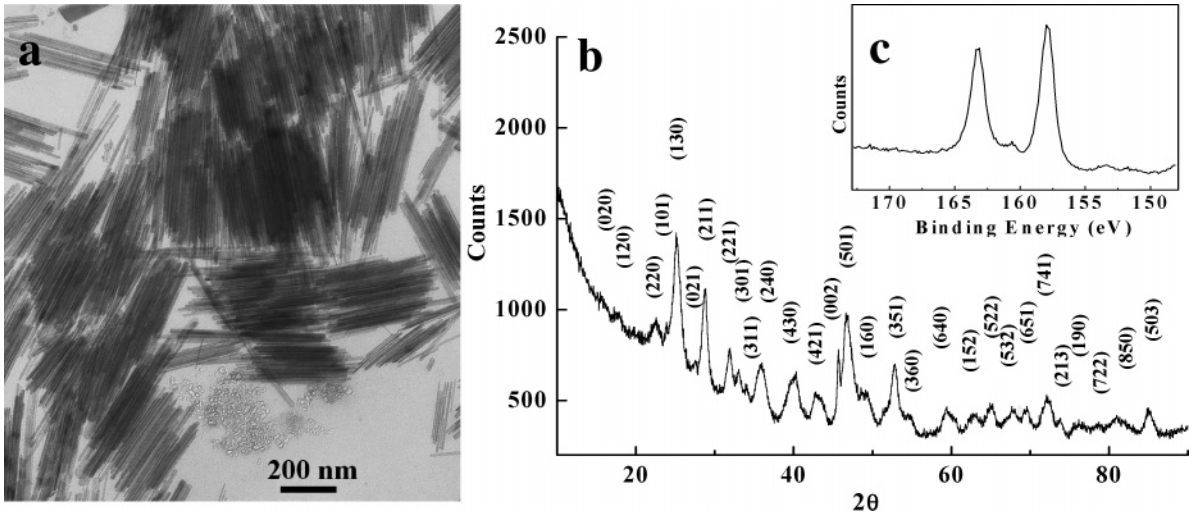

Figure 1. (a) Typical TEM image of Bi_2S_3 nanorods. (b) XRD pattern of the product. (c) XPS spectrum of close-up survey for Bi 4f core.

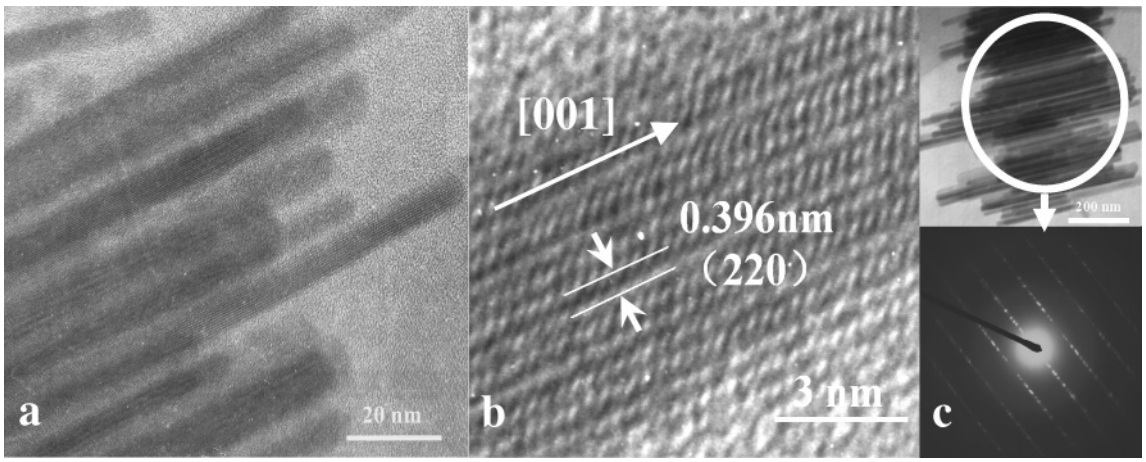

Figure 2. (a) HRTEM image of Bi_2S_3 nanorods. (b) HRTEM image of a typical Bi_2S_3 nanorod. (c) SAED pattern of a bundle of parallel Bi_2S_3 nanorods.

163.3 eV, respectively, which confirm the presence of the corresponding elements for Bi_2S_3 nanorods.[14a]

Figure 2 show the typical HRTEM images of the Bi_2S_3 nanorods, the single Bi_2S_3 nanorod and the selected area electron diffraction (SAED) corresponding to a bundle of parallel nanorods. It can be found that each nanorod shows clear crystal lattice fringes from Figure 2a. In accordance with the XRD analysis, the HRTEM and the SAED pattern may also be indexed to the orthorhombic phase of Bi_2S_3 (JCPDS 17-320). The SAED pattern taken along the [220] zone axis reveals that the nanorods are single-crystalline in nature. Figure 2b reveals that the nanorods are highly crystallized, free from dislocation and stacking faults. The observed lattice spacing of 0.396 nm correspond to the (220) planes. Both the HRTEM image and the SAED pattern show that the nanorods grow along the [001] direction, which is shown with the white arrow in Figure 2b.

To further study the growth process of Bi_2S_3 nanorods, we performed a series of experiments under the same conditions except for reaction time, and the results are shown in Figure 3. It is clear that only small, irregular-shaped particles with an average diameter of 7 nm and aspect ratio of less than 3 emerge when the reaction time is 1 min (Figure 3a). XPS analysis on this product also reveals that the banding energy of Bi $4f_{7/2}$ and $4f_{5/2}$ peaks are 158.0 and 163.3 eV, respectively, indicating that they are Bi_2S_3 particles. Their XRD and SAED patterns exhibit broad peaks and indistinct diffusion rings, corresponding to small crystallites. These peaks and rings are somewhat ambiguous, but could still be assigned to the orthorhombic Bi_2S_3 phase. When the reaction time is prolonged to 3 min, rodlike particles with an average diameter of 8 nm and aspect ratio of about 5 begin to emerge among the irregular-shaped particles (Figure 3b). The corresponding XRD and SAED patterns exhibit more clear peaks and rings. When the reaction time is prolonged to 10 min, large numbers of rodlike Bi_2S_3 particles with an average diameter of 8 nm and an average length of 50 nm (Figure 3c) come into existence. When the reaction duration is 1 h, well-crystallized nanorods with a higher aspect ratio are produced, but there are still a few of Bi_2S_3 nanoparticles (Figure 3d). When the reaction time was longer than 1.5 h, large quantities of uniform Bi_2S_3 nanorods with high aspect ratios have been fully formed (images e and f of Figure 3). The morphologies of the products have no obvious difference when the reaction continues for an excess of several hours. These results reveal that the formation of Bi_2S_3 nanorods may be attributed to the growth or integration of Bi_2S_3 nanocrystallites along its [001] direction under this solvo-

(14) (a) Debies, T. P.; Rabalais, J. W. *Chem. Phys.* **1977**, *20*, 277.(b) Vasquez, R. P.; Grunthaner, F. J. *J. Appl. Phys.* **1981**, *52*, 3509.

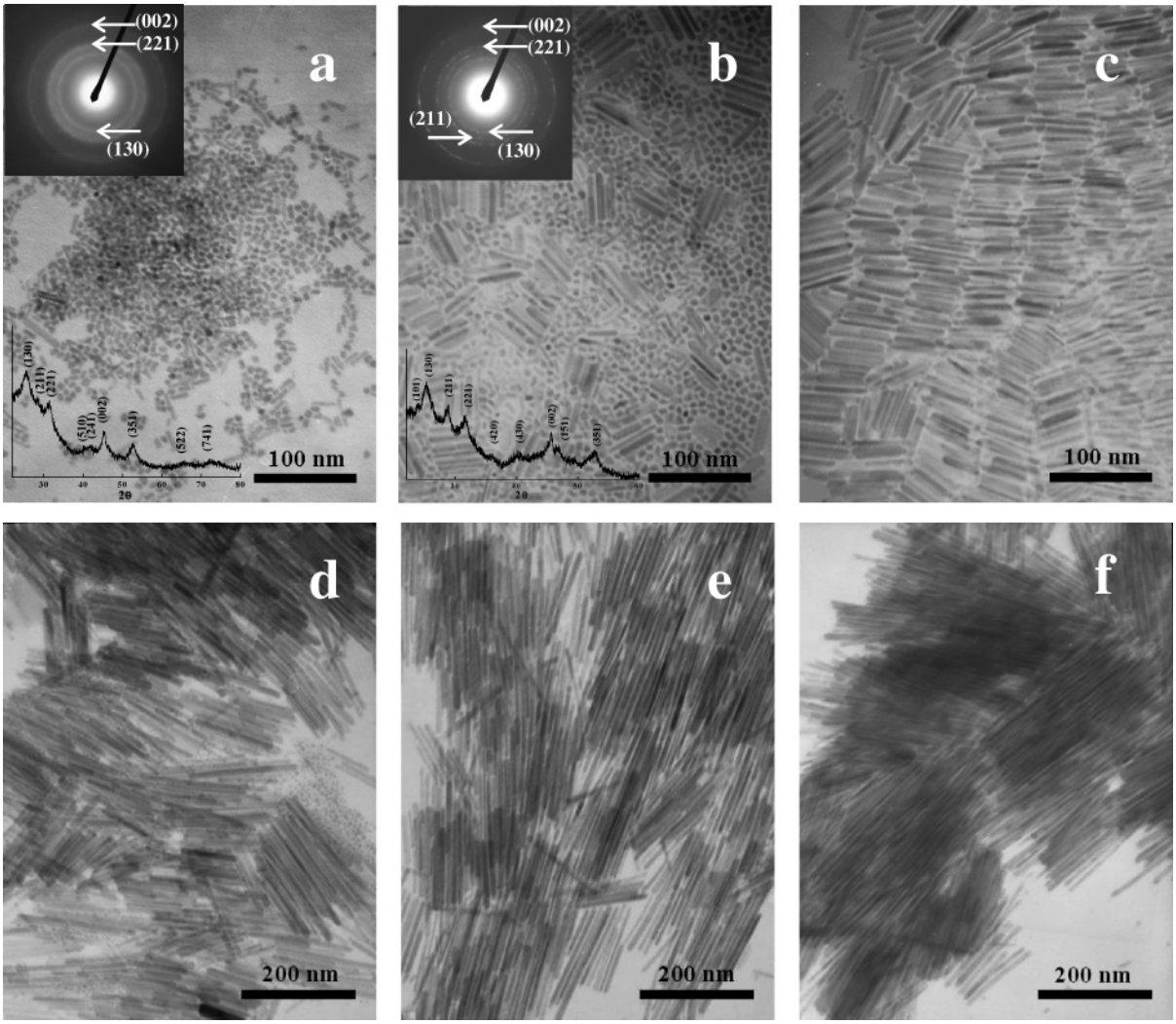

Figure 3. TEM images of Bi_2S_3 products obtained under the same concentration of precursors in oleylamine at 160 °C for (a) 1, (b) 3, (c) 10, (d) 60, (e) 100, and (f) 300 min. Inserts in upper-left of parts a and b give the corresponding SAED patterns and inserts in the lower-left give the corresponding XRD patterns.

Scheme 1. Supposed Formation Process of the Bi_2S_3 Nanorods Prepared by the Solvothermal Decomposition of the Single Source Precursor

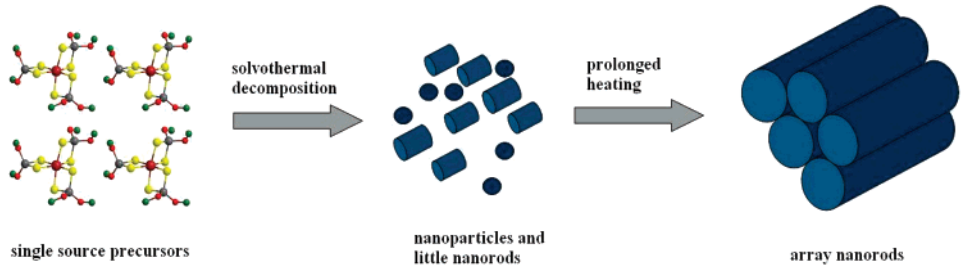

thermal condition. A supposed formation process of the Bi_2S_3 nanorods is described in Scheme 1.

We speculate that a suitable solvothermal condition may be helpful for the nucleation and subsequent preferential growth of Bi_2S_3 nanorods. The effects of the reaction temperature and concentration of the precursor have been also explored. A series of preparation experiments at different reaction temperature are conducted by heating the solution of $Bi[S_2P(OC_8H_{17})_2]_3$ in oleylamine for 5 h at 120, 140, 160, and 180 °C, respectively. When the reaction temperature is 120 °C, the color of the solution changes from transparent green to dark-gray slowly, indicating the decomposition of the precursor is inefficient at this condition. TEM analysis of the final product reveals that only irregular-shaped nanoparticles rather than nanorods are produced. At higher temperature, the transition of the solution color is greatly accelerated. The solution turns dark after several minutes at 140 °C, a few seconds at 160 °C, and almost immediately at 180 °C, respectively. These observations indicate that an efficient preparation could be achieved under an appropriately high reaction temperature. Figure 4 shows the TEM photos of the corresponding final products. It is clear that the rodlike Bi_2S_3 crystals with lengths of 250−450 nm and an average diameter of 21 nm begin to come forth (Figure 4c) at 140

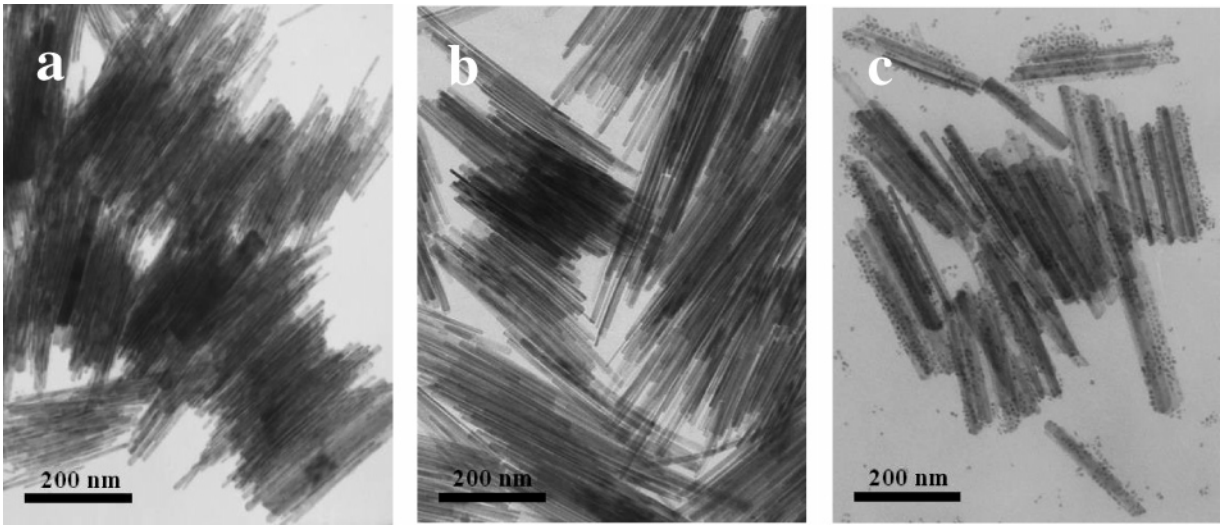

Figure 4. TEM images of Bi_2S_3 products obtained by thermal decomposition of the same concentration of the precursors in oleylamine at different reaction temperatures for 5 h: (a) 180, (b) 160, and (c) 140 °C.

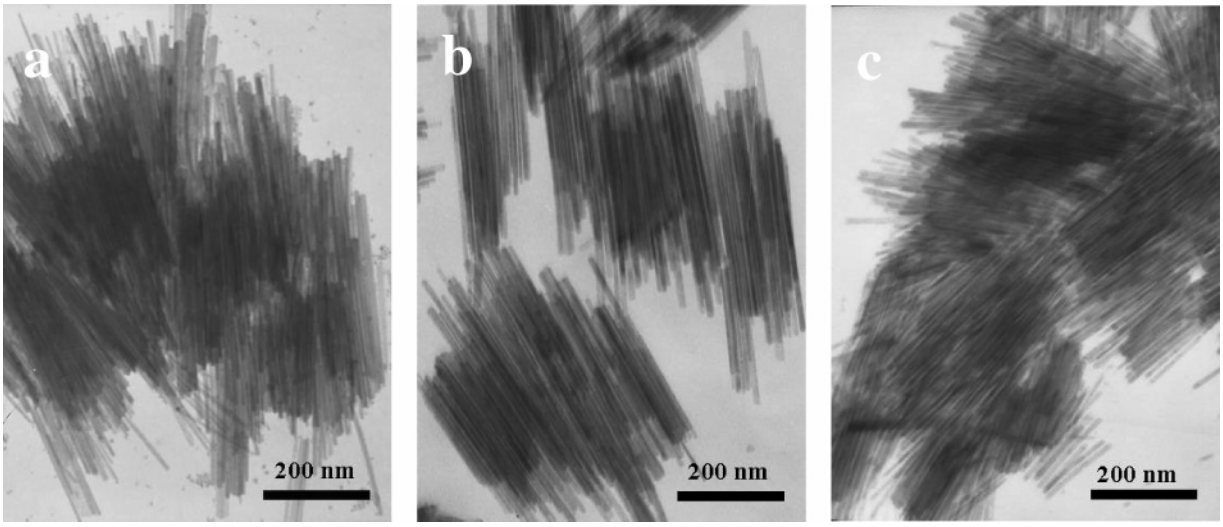

Figure 5. TEM images of Bi_2S_3 products obtained by solvothermal decomposition of (a) 0.13 g (0.1 mmol), (b) 0.25 g (0.2 mmol), and (c) 0.39 g (0.3 mmol) of precursor dissolved in 5 g of oleylamine at 160 °C for 5 h.

°C. However, there are many nanoparticles at the same time, indicating that the formation of rodlike nanomaterials is inadequate at this condition. When the reaction temperature is 160 °C, Bi_2S_3 nanorods with lengths of 300−550 nm and an average diameter of 11 nm are prepared. These nanorods give a more clear morphology in TEM photo, and irregular-shaped nanoparticles could not be found any more. At 180 °C, Bi_2S_3 nanorods with lengths of 300−600 nm and an average diameter of 8 nm are prepared. According to the analysis of these results, we conclude that the higher reaction temperatures, such as 160−180 °C, are suitable for the efficient preparation of Bi_2S_3 nanorods. We also found a slight increase in length and decrease in diameter of the product when the reaction temperature was elevated.

The influences of the concentration of the precursor on the Bi_2S_3 morphology have also been investigated. Figure 5 show the TEM images of the various Bi_2S_3 nanorods prepared by varying the concentration of the precursor while other conditions are fixed. It is found that the morphology of as-prepared Bi_2S_3 has no obvious change in the investigated concentration range, which still exhibits rodlike shape, and the diameter of the Bi_2S_3 nanorods has no distinct change. But the length of the Bi_2S_3 nanorods decreases with increasing concentration of the precursor. The reason could be explained as follows. When the concentration is higher, it is much easier to generate transient super-saturation in monomers and induce a nucleation burst when the temperature of this system reaches to a threshold value.[15] That is to say the higher concentration of the precursor can afford more "growing seeds" during the earlier stage of reaction process. A rapid and intense nucleation burst will lower the precursor concentration below the nucleation threshold, and all "seeds" have the coequal chance to grow into nanorods or be depleted by others. The product of the thermal decompose of $Bi[S_2P(OC_8H_{17})_2]_3$ has obvious preferential growth orientation under these experimental conditions. So the higher the precursor's concentration, the shorter the length of the Bi_2S_3 nanorods.

It is feasible to prepare other V−VI semiconductors nanomaterials by solvothermal decomposition of the corresponding metal dialkyldithiophosphate complexes. When the precursor is replaced with antimony di-*n*-octyl-dithiophos-

(15) Yin, Y. D.; Alivisatos, A. P. *Nature* **2005**, *437*, 664.

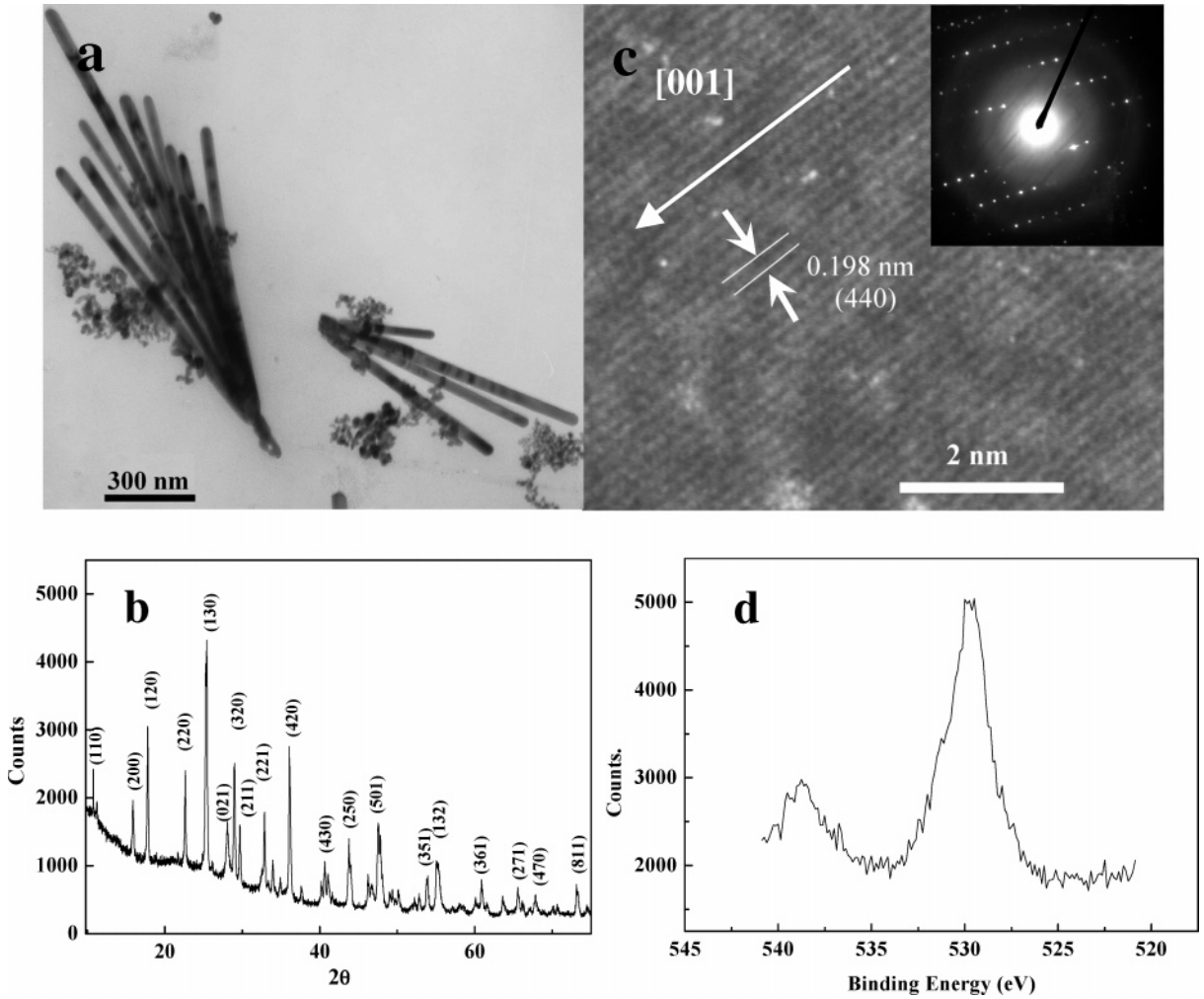

Figure 6. (a) Typical TEM image of Sb_2S_3 nanorods. (b) XRD pattern of the product. (c) HRTEM image of a single Sb_2S_3 nanorod. The insert is the corresponding SAED pattern. (d) XPS spectrum of close-up survey for Sb 3d core.

phates, Sb_2S_3 nanorods can be obtained. Figure 6a shows the TEM image of uniform Sb_2S_3 nanorods with a length of 1 μm $\pm$ 100 nm and a diameter of 45 $\pm$ 5 nm, along with some irregular nanoparticles. The XRD pattern of the product is shown in Figure 6b, in which the diffraction peaks can be fully indexed to the orthorhombic phase of Sb_2S_3 (cell constants $a = 11.23$ Å, $b = 11.31$ Å, $c = 3.841$ Å; JCPDS card file 42-1393). A further conformation of the Sb_2S_3 nanorods structure is obtained in Figure 6c, which shows the HRTEM image and corresponding SAED pattern of the single Sb_2S_3 nanorod. Like the XRD profile, the HRTEM and SAED patterns may also be indexed as the orthorhombic phase of Sb_2S_3 (JCPDS 42-1393). The lattice spacing of about 0.198 nm corresponds to the (440) planes spacing of orthorhombic phase of Sb_2S_3. The SAED pattern taken along the [220] zone axis is a spot pattern, revealing that the Sb_2S_3 nanorods are also single-crystalline in nature. Both the HRTEM and SAED pattern demonstrate that the nanorod grows along [001] direction indicated with an arrow in Figure 6c, which coincides with that of the above prepared Bi_2S_3 nanorods. The formation of Sb_2S_3 is further proved by XPS analysis (Figure 6d). The Sb $3d_{5/2}$ and $3d_{3/2}$ peaks are observed at 529.8 and 538.9 eV, which are consisted with the previously reported values of antimony sulfides in the literature.[14b]

An optical absorption experiment has been carried out using the UV−visible absorption spectra, which provide a simple and effective method for explaining some features concerning the band structure. Figure 7 show the typical UV−visible absorption spectra taken from Bi_2S_3 and Sb_2S_3 nanorods. The corresponding band gap values are obtained by the intersection point of the tangent of the absorption edge with extended line of the absorption at lower wavelengths. Readily observable in Bi_2S_3 nanorods (Figure 7a) is an ~0.4 eV blue shift in the absorption edge relative to the band gaps in the bulk materials.[16] Such obvious blue shifts are consistent with the confinement of charge carriers in microcrystallites with at least one dimension comparable to the Bohr radius of electron−hole pairs in the bulk solid. For the Sb_2S_3 sample (Figure 7b), there are one weak peak of 2.22 eV that is due to the nanoparticles dispersed around nanorods, and one shoulder peak of 1.76 eV (signed with "*") that is due to the nanorods. Our Sb_2S_3 nanorods are mainly about 45 nm $\times$ 1 μm in size (according to the analysis of TEM image), and we do not expect the corresponding E_g to be very different from that of bulk materials. The experimentally determined E_g values of Bi_2S_3 and Sb_2S_3 nanorods are near

(16) Variano, B. F.; Hwang, D. M.; Sandroff, C. J.; Wiltzius, P.; Jing, T. W.; Ong, N. P. *J. Phys. Chem. B* **1987**, *91*, 6455.

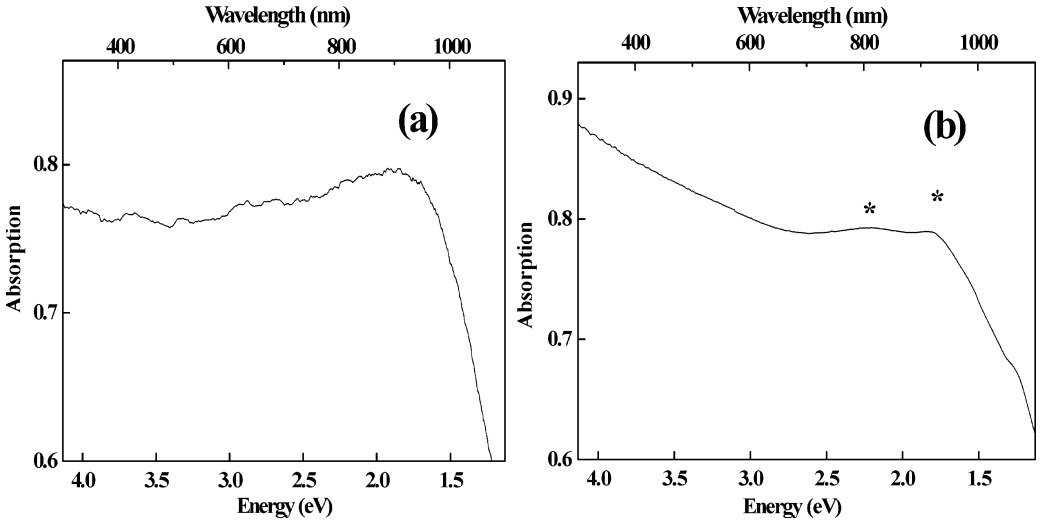

Figure 7. Experimental UV−visible spectra taken from (a) Bi_2S_3 nanorods and (b) Sb_2S_3 nanorods.

to the optimum for photovoltaic conversion, suggesting that they may be very promising for applications in solar energy and photoelectronics.

4. Conclusion

In conclusion, high-quality single-crystal nanorods of Bi_2S_3 and Sb_2S_3 have been successfully prepared by a one-pot solvothermal process characterized by the use of $Bi[S_2P(OC_8H_{17})_2]_3$ and $Sb[S_2P(OC_8H_{17})_2]_3$ as novel single-source precursors. This approach offers a great deal of control of the size and the morphology of M_2S_3 nanomaterials and facilitates their production at a relative low-reaction temperature without the need of protection by inert gases or sealed containers. In this process, the preparation conditions such as reaction time, temperature, and concentration of the precursors have an obvious effect on the size and aspect ratio of the product, which could be utilized to tailor the morphology of this useful material on the nanoscale level. Furthermore, the resulting productions are as small as 10 nm at least in one dimension, which is close to their Bohr radius, and can thus exhibit obvious quantum confinement effects that would stimulate important applications in energy conversion and photoelectronics.

Acknowledgment. This work is supported by the National Natural Science Foundation of China (Grant 20473106), the Ministry of Science and Technology (973 Grant 2007CB607601), and Technology and Innovation Group (Grant 50421502).

CM062549O